OPEN BIOLOGY

royalsocietypublishing.org/journal/rsob

Research

Cite this article: York-Andersen AH, Wood BW, Wilby EL, Berry AS, Weil TT. 2021 Osmolarity-regulated swelling initiates egg activation in *Drosophila*. *Open Biol.* **11**: 210067. https://doi.org/10.1098/rsob.210067

Received: 17 March 2021
Accepted: 22 June 2021

Subject Area:
developmental biology

Keywords:
Drosophila, osmolarity, calcium wave, egg activation

Author for correspondence:
Timothy T. Weil
e-mail: tw419@cam.ac.uk

THE ROYAL SOCIETY PUBLISHING

Osmolarity-regulated swelling initiates egg activation in *Drosophila*

Anna H. York-Andersen, Benjamin W. Wood, Elise L. Wilby, Alexander S. Berry and Timothy T. Weil

Department of Zoology, University of Cambridge, Downing Street, Cambridge CB2 3EJ, UK

TTW, 0000-0003-0490-849X

Egg activation is a series of highly coordinated processes that prepare the mature oocyte for embryogenesis. Typically associated with fertilization, egg activation results in many downstream outcomes, including the resumption of the meiotic cell cycle, translation of maternal mRNAs and cross-linking of the vitelline membrane. While some aspects of egg activation, such as initiation factors in mammals and environmental cues in sea animals, have been well-documented, the mechanics of egg activation in insects are less well-understood. For many insects, egg activation can be triggered independently of fertilization. In *Drosophila melanogaster*, egg activation occurs in the oviduct resulting in a single calcium wave propagating from the posterior pole of the oocyte. Here we use physical manipulations, genetics and live imaging to demonstrate the requirement of a volume increase for calcium entry at egg activation in *ex vivo* mature *Drosophila* oocytes. The addition of water, modified with sucrose to a specific osmolarity, is sufficient to trigger the calcium wave in the mature oocyte and the downstream events associated with egg activation. We show that the swelling process is regulated by the conserved osmoregulatory channels, aquaporins and DEGenerin/Epithelial Na^+ channels. Furthermore, through pharmacological and genetic disruption, we reveal a concentration-dependent requirement of transient receptor potential M channels to transport calcium, most probably from the perivitelline space, across the plasma membrane into the mature oocyte. Our data establish osmotic pressure as a mechanism that initiates egg activation in *Drosophila* and are consistent with previous work from evolutionarily distant insects, including dragonflies and mosquitos, and show remarkable similarities to the mechanism of egg activation in some plants.

1. Introduction

Egg activation is a conserved process that prepares a mature oocyte for embryogenesis. It actuates many essential cellular processes including the resumption of meiosis, modification of the outer membrane, post-transcriptional regulation of maternal mRNAs and broad changes in the cytoskeletal environment [1–3]. This process requires a transient increase of intracellular calcium, often referred to as a calcium wave(s), with multiple waves observed in mammals and ascidians, compared to a single wave in *Xenopus laevis*, *Danio rerio* and *Drosophila melanogaster* [4–6].

Species variation is also documented in the initiation mechanism and source of calcium required for the cytoplasmic rise [1,4]. In vertebrates and some invertebrates, egg activation is dependent on fertilization in which sperm entry introduces phospholipase C enzymes generating a calcium efflux from the endoplasmic reticulum [2,7]. Comparatively, egg activation in other invertebrates can be independent of fertilization and initiated by external factors [8]. For example, the ionic composition of the solution external to the oocyte is required in the starfish *Asterina pectinifera*, as chelation of sodium ions in

seawater disrupted the resumption of meiosis [9,10]. While in the shrimp *Siconia ingentis*, egg activation requires the presence of magnesium ions in seawater [11]. Interestingly, in the stick insect *Catrausius morosus*, exposure of the oocyte to oxygen in the air results in the resumption of meiosis [12].

An alternative external cue of egg activation is the application of mechanical pressure on the oocyte plasma membrane exemplified by the eggs of the wasp *Pimpla turionellae*, which are activated when squeezed through a polythene capillary [13,14]. This physical stress is proposed to displace the maternal nucleus and result in the resumption of the cell cycle. Similarly, the eggs of *D. mercatorum* are thought to be activated by the pressure from the genital ducts [12]. Tension in the plasma membrane can also be generated by a change in the osmolarity of the external solution (which we will refer to as 'osmotic pressure' henceforth). Prior to egg activation, the hypertonic environment in the ovaries is thought to maintain the oocytes in a meiotically arrested state [15,16]. Subsequent entry of the oocyte into a hypotonic environment results in the egg activation of dragonfly, mayfly, turnip sawfly and yellow fever mosquito eggs [16–18]. For instance, upon entry into water, yellow fever mosquito oocytes undergo a visible darkening due to the increased production and cross-linking of the endochorion at egg activation [19,20]. Overall, physical pressure appears to be a conserved mechanism for initiating egg activation in many insects.

Similar to other insects, egg activation in *D. melanogaster* is independent of fertilization and occurs during the passage of the mature oocyte through the oviduct [21]. One model suggests that the pressure exerted by the oviduct on the oocyte upon entry initiates the calcium wave at egg activation [15,22]. An experiment supporting this model applied pressure by laying a coverslip on top of the mature oocyte, leading to the generation of a calcium wave [6]. An alternative approach showed that the application of pressure through passing the mature oocyte into a narrow capillary was not sufficient to trigger a calcium rise or wave [5].

A second model proposes that osmotic pressure generated by uptake of oviduct fluid leads to the initiation of egg activation [15]. This is supported by observations that oocytes are visibly dehydrated while in the ovaries, but upon deposition appear turgid and hydrated [15,23]. Rehydration at egg activation can be recapitulated *ex vivo* through the addition of a hypotonic solution, known as activation buffer (AB), which when added to an isolated mature egg results in swelling and a single calcium wave [5,6,15]. This influx of calcium requires the transient receptor potential M (Trpm) mechanosensitive channel in the plasma membrane and results in the activation of Plc21C that sustains the wave [8,24,25]. Regulation of calcium entry was hypothesized to be related to the distribution of the Trpm protein in the membrane, as calcium entry is often seen first at the poles. However, when observed using an antibody against the endogenous Trpm, an even distribution of the protein across the plasma membrane was evident [26]. Therefore, the precise mechanisms of initiation and regulation of the calcium wave remain to be elucidated in *Drosophila*.

Here, we use live imaging in conjunction with novel physical manipulation, pharmacological disruption and genetics, to demonstrate the requirement of osmotically induced swelling for calcium entry and downstream events of *Drosophila* egg activation. We show that depletion of osmoregulatory machinery, including aquaporins (AQPs) and DEGenerin/Epithelial Na^+ (DEG/ENaC) channels, disrupts water homeostasis and egg activation. We provide further evidence that the movement of calcium ions into the egg is sensitive to levels of functional Trpm. Our data also argue that the external environment is not the source of calcium for the wave, but rather the ions are likely to originate from the perivitelline space. Together with other recent work in the field, our findings reveal that *Drosophila* egg activation has striking mechanistic similarities to other animals and even some plants.

2. Results

2.1. Swelling is required for the initiation and propagation of the calcium wave *ex vivo*

The likely initiation cues for the calcium wave at *Drosophila* egg activation include physical pressure applied on the posterior pole by the oviduct or the uptake of the fluid by the mature oocyte from the oviduct [8,15]. Our previous work has shown that physical pressure applied to the posterior pole is not sufficient to initiate the calcium wave [5,27]. This evidence, together with the observation that the mature oocytes are dehydrated while in the ovary but are turgid by the time they are deposited [15], suggests that swelling might play a role in the initiation and the propagation of the calcium wave at egg activation.

In addition to the initiation of the calcium wave, *ex vivo* dissected mature oocytes show an increase in oocyte volume, rounding of the oocyte poles and movement of the dorsal appendages following exposure to AB (figure 1*a*). To test if this swelling is required for the initiation and propagation of the calcium wave, we blocked the ability of the egg to swell by placing the anterior pole in a plastic capillary with the posterior pole being exposed to oil (figure 1*b*). Upon the addition of AB, the oil is displaced and the calcium wave initiated as normal. However, the wave did not propagate past the opening of the capillary (figure 1*b*′). An uninhibited calcium wave would normally encompass the whole oocyte by 3.5 min [5]. However, in this case, the wave did not propagate until the egg was expelled from the capillary. When the whole oocyte was placed in the capillary, as expected, the calcium wave did not initiate upon the addition of AB (data not shown). This strongly suggests that swelling is required for the initiation and propagation of the calcium wave.

Our previous work has shown that local pressure or injection of calcium gives a localized calcium increase, but not a prolonged or broad calcium increase in the form of a wave [5,27]. To test if a localized internal increase in volume could induce a broad calcium event, we used a microneedle to inject halocarbon oil into a mature egg chamber mounted in halocarbon oil. Initial puncturing of the egg chamber resulted in a localized increase in calcium consistent with our previous results (figure 1*c*; $t = 0'$). Injection of oil into the centre of the egg chamber resulted in a broad posterior calcium increase (figure 1*c*; $t = 1', 2'$). This response is noticeably different from previous experiments where oocytes were manipulated with a microneedle or had physical pressure applied. These data suggest swelling is necessary for calcium propagation and is sufficient for the initiation of a broad calcium increase.

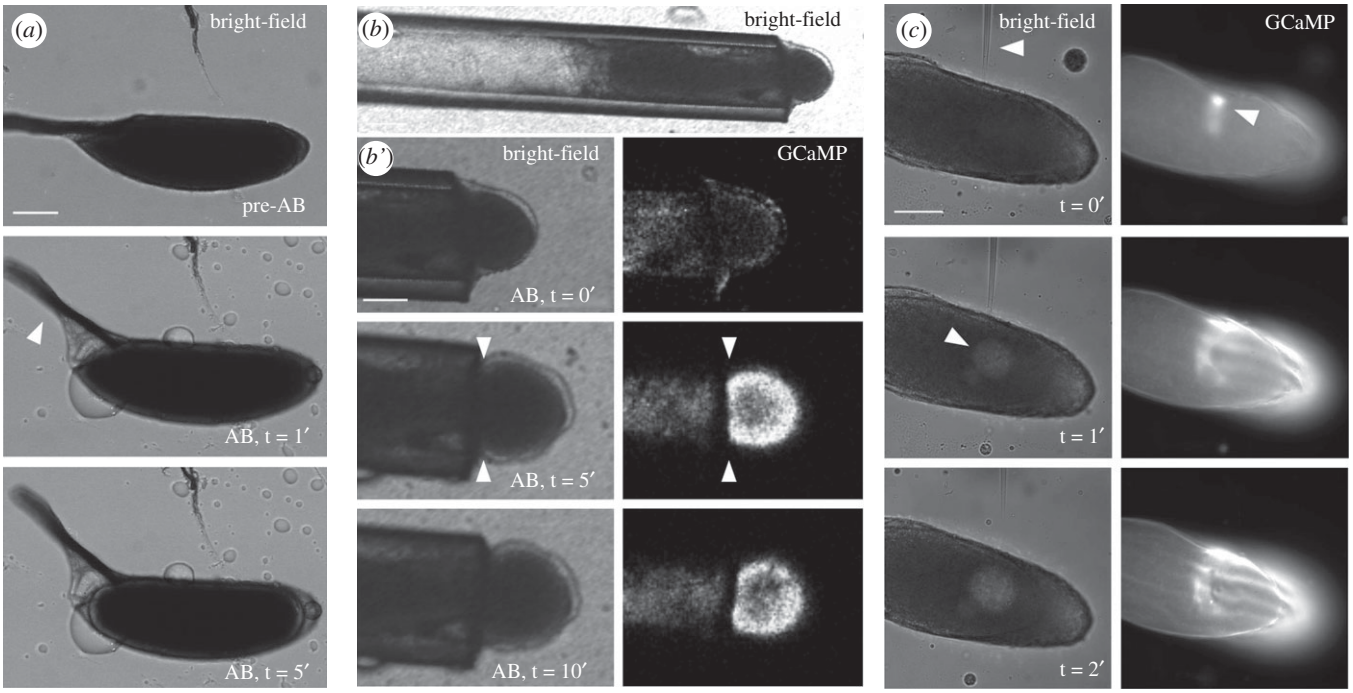

Figure 1. Egg chamber swelling is required for the initiation and propagation of the calcium wave. Time series showing *ex vivo* mature egg chambers imaged with bright-field or fluorescence (*a*,*b*,*b*′,*c*) and expressing *UAS-myrGCaMP5* (*b*,*b*′,*c*). Images represent a single plane. (*a*) Time series of a wild-type egg chamber pre- and post-addition of AB. Upon the addition of AB, the egg chamber undergoes swelling, the dorsal appendages rise (white arrowhead, $t = 1'$) and the poles become more rounded (white arrow, $t = 5'$). Circular droplets visible on the outside of the egg are oil that was not displaced by AB. Scale bar 100 µm. (*b*) Bright-field image of an egg chamber, expressing *UAS-myrGCaMP5*, placed in a 125 µm diameter tube. (*b*′) Time series of the same egg chamber in the tube, with the posterior pole exposed to AB. The calcium wave initiates normally but does not propagate past the tube opening (white arrowheads) ($n = 15$). Scale bar 60 µm. (*c*) Bright-field image of a mature egg chamber, expressing *UAS-myrGCaMP5*, injected with halocarbon oil. As the needle enters the oocyte, there is a calcium increase at the point of injection (white arrowhead, $t = 0'$). Injected oil is seen as a circle in the cytoplasm of the egg at $t = 1'$ (white arrowhead) and remains localized ($t = 2'$). Localized swelling results in an increase in calcium, which does not propagate ($t = 2'$) ($n = 5$). Scale bar 100 µm.

2.2. Osmotic pressure initiates a calcium wave *ex vivo*

In order to further test the function of swelling, we established a classification system that enabled us to categorize calcium events in the egg and quantify our data under different experimental conditions. We have classified the calcium increase exhibited as four distinct phenotypes: full-wave, cortical increase, partial wave or no wave. The most common phenotype is the full-wave that initiates from the posterior pole and propagates across an entire oocyte. This is the standard event that we observe with *ex vivo* egg activation using AB. We do observe a small percentage of full-wave phenotypes that initiate from the anterior pole. Different to a full-wave, an increase in calcium can occur from multiple places around the cortex. This cortical increase phenotype was originally observed when egg chambers were exposed to distilled water [5]. These observations suggest that all parts of the egg have the capacity to allow calcium into the cell and that there is a regulatory mechanism to control calcium entry. By contrast, the partial wave phenotype describes the calcium wave that initiates from a pole but does not propagate across the entire oocyte and recovers prematurely. We do observe some egg chambers attempting to initiate waves multiple times, without successful propagation of calcium. Finally, the no wave phenotype describes an absence of a calcium increase anywhere in the egg for the length of the experiment. We observe this in a small percentage of eggs that are likely to have a major defect in development prior to dissection.

Our data indicate the requirement of swelling for the calcium wave to occur at egg activation (figure 1*b*). One way the egg could undergo swelling is by exposure to a hypotonic solution, which would cause an influx of water and subsequently generate osmotic pressure within the mature oocyte. To test whether or not the uptake of water alone could act as an initiation cue for the calcium wave at egg activation, *ex vivo* egg chambers were treated with a sucrose and water solution (SW) of the same solute content as AB, measured in osmolarity (260 mOsm). The SW solution has no ions added and is very different from other buffers used to activate eggs. Sucrose is highly soluble in water and is neutrally charged making it suitable for varying the osmolarity of the solution. Upon the addition of SW, the egg chambers exhibited a similar proportion of the calcium wave phenotypes to AB (figure 2*a*).

To further test whether the osmolarity of an external solution is important for the initiation of an internal calcium increase, egg chambers were exposed to a single SW solution from a range of osmolarities. The highest percentage of full-calcium waves was observed at 350 mOsm, with this percentage declining rapidly by 570 mOsm (figure 2*a*′). The highest proportion of cortical increases was detected at 0 mOsm (figure 2*a*′), consistent with predictions that an excessive volume increase cannot be regulated by the egg and results in an uncontrolled calcium increase. The partial and no wave phenotypes became more predominant with an increase in the osmolarity. This suggests that high-osmolarity solutions do not increase the internal volume that is required for the egg to complete a calcium event. Together, these findings suggest that a controlled amount of water entering the egg is important for regulating a calcium event at egg activation.

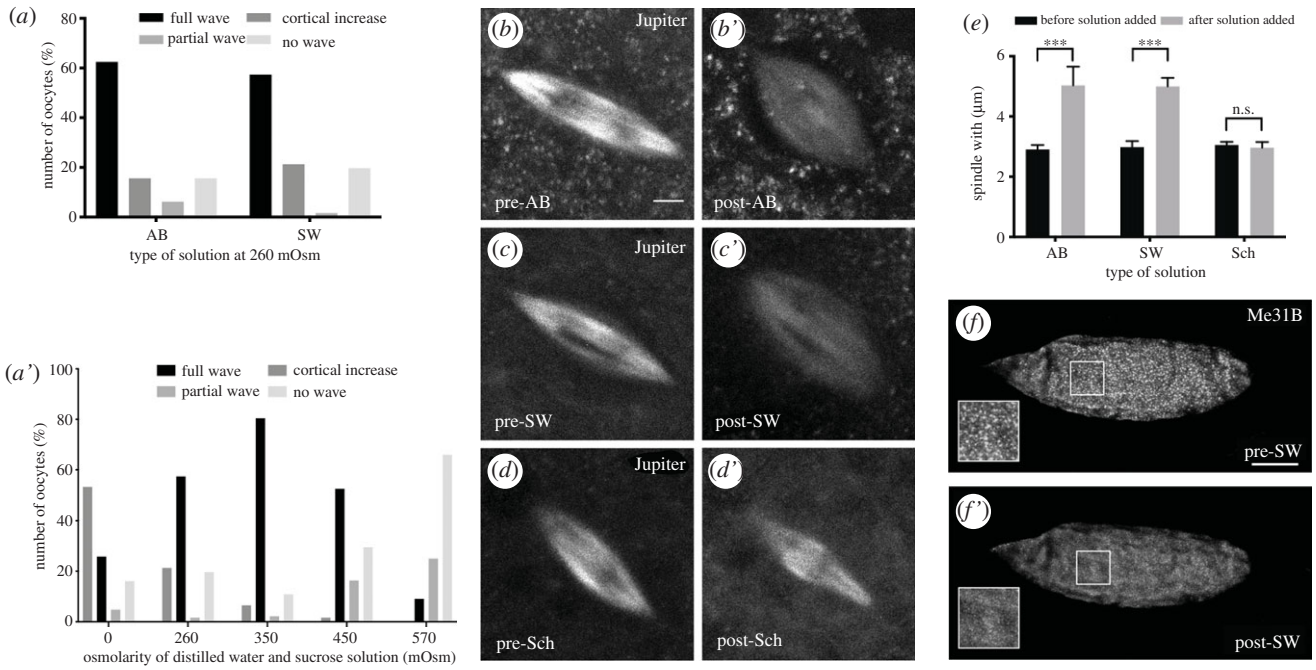

Figure 2. Osmotic pressure initiates the calcium wave and results in rearrangement of the meiotic spindle and P body dispersion. (*a*) Data showing AB or sucrose and water (SW) of 260 mOsm results in a similar percentage of the calcium wave phenotypes when added to *ex vivo* egg chambers. (*a*′) The data show the number of mature oocytes activated with SW only, with a range of osmolarities from 0–570 mOsm. The number of full waves increases from 0 mOsm, peaks at 350 mOsm and then decreases with higher osmolarities. The proportion of egg chambers that show a cortical increase peaks at 0 mOsm and then decreases with higher osmolarities. The proportion of partial waves increases with higher osmolarities. The proportion of no wave increases with higher osmolarities ($n = 30$ per osmolarity). These data were analysed statistically using Fisher's exact test with $p < 0.05$ considered significant. The proportion of full calcium waves observed at 350 mOsm is significantly higher ($p < 0.05$) than full waves at all other osmolarities shown. The proportion of cortical increases observed at 0 mOsm is significantly higher ($p < 0.01$) than cortical increases at all measured osmolarities shown. The proportion of partial waves observed at 570 mOsm is significantly higher ($p < 0.01$) than partial waves at all measured osmolarities, except 450 mOsm. The proportion of no waves observed at 570 mOsm is significantly higher ($p < 0.001$) than no waves at all other osmolarities shown. (*b–d*′) Mature *ex vivo* egg chambers expressing *jupiter-mCherry* to visualize microtubules in the meiotic spindle. Before activation (pre) the spindle is in the shape of an ellipse, with dark regions in the middle where the DNA resides (*b–d*). Post-incubation images were taken 10 min after the addition of the solution. The spindle shows an increase in width following the addition of AB and SW (260 mOsm) (*b,c*′), however, the width does not change upon the addition of Schneider's *Drosophila* Medium (Sch) ($n = 15$). Scale bar 2 µm. Maximum projection 3 µm. (*e*) Graph showing a change in spindle width upon addition of AB, SW and Sch. The data were analysed statistically using an unpaired *t*-test with $p < 0.05$ considered significant. The spindle shows a significant increase in width by 2.1 µ (a 1.7× increase) ($p < 0.001$) upon the addition of AB or SW (260 mOsm). There is no significant change in width upon the addition of Sch ($n = 15$ per solution). (*f–f*′) Time series of *ex vivo* egg chamber expressing *me31B::GFP* following the addition of SW (260 mOsm). P bodies appear as granular puncta pre-SW and disperse following the addition of SW, consistent with the addition of AB ($n = 15$). Post-incubation images were taken at 20 min after incubation of solution. Scale bar 60 µm. Maximum projection 40 µm.

2.3. Osmotic pressure results in the resumption of the meiotic cell cycle *ex vivo*

Previous work has shown that the addition of AB to mature egg chambers can initiate major cellular events associated with *Drosophila* egg activation, including the resumption of the cell cycle and processing bodies (P bodies) dispersion [5,28]. In a non-activated oocyte, the meiotic spindle is parallel to the cortex and is observed near the base of the dorsal appendages at the anterior pole [28–30]. Upon egg activation, the spindle undergoes a morphological change within 10 min, marking the resumption of the cell cycle [28].

To address whether osmotic pressure can result in this change, we used Jupiter-mCherry to label the meiotic spindle and exposed these mature egg chambers to SW solution (260 mOsm). Before exposure, the spindle is a narrow ellipse with dark regions in the middle where the DNA resides (figure 2*b–d*). Upon addition of SW and AB (positive control), the spindle shows a significant increase in width (70%), which is indicative of spindle contraction at anaphase I (figure 2*b*,′*c*′,*e*). When treated with Schneider's *Drosophila* medium (negative control), the spindle did not undergo any detectable morphological change (figure 2*d*′,*e*). Together, this supports the conclusion that water uptake and subsequent internal pressure are sufficient to initiate the metaphase I to anaphase I transition of the meiotic spindle.

To further verify the role of osmotic pressure, we investigated the dispersion of P bodies, an established hallmark of egg activation [5,31]. When mature egg chambers expressing a conserved P-body marker are exposed to SW (260 mOsm), we observe a normal dispersion phenotype (figure 2*f–f*′). Taken together, these data suggest that an increase in internal volume caused by osmotic pressure triggers downstream events of *ex vivo* egg activation.

2.4. Water homeostasis is required for egg activation

The increase in internal volume observed in osmolarity experiments is regulated by water influx and efflux. To test if water homeostasis is required to regulate swelling in mature oocytes, we explored the role of the water-pore channels, AQPs, which are known to coordinate the movement of water molecules [32,33]. By adding copper sulfate (a broad

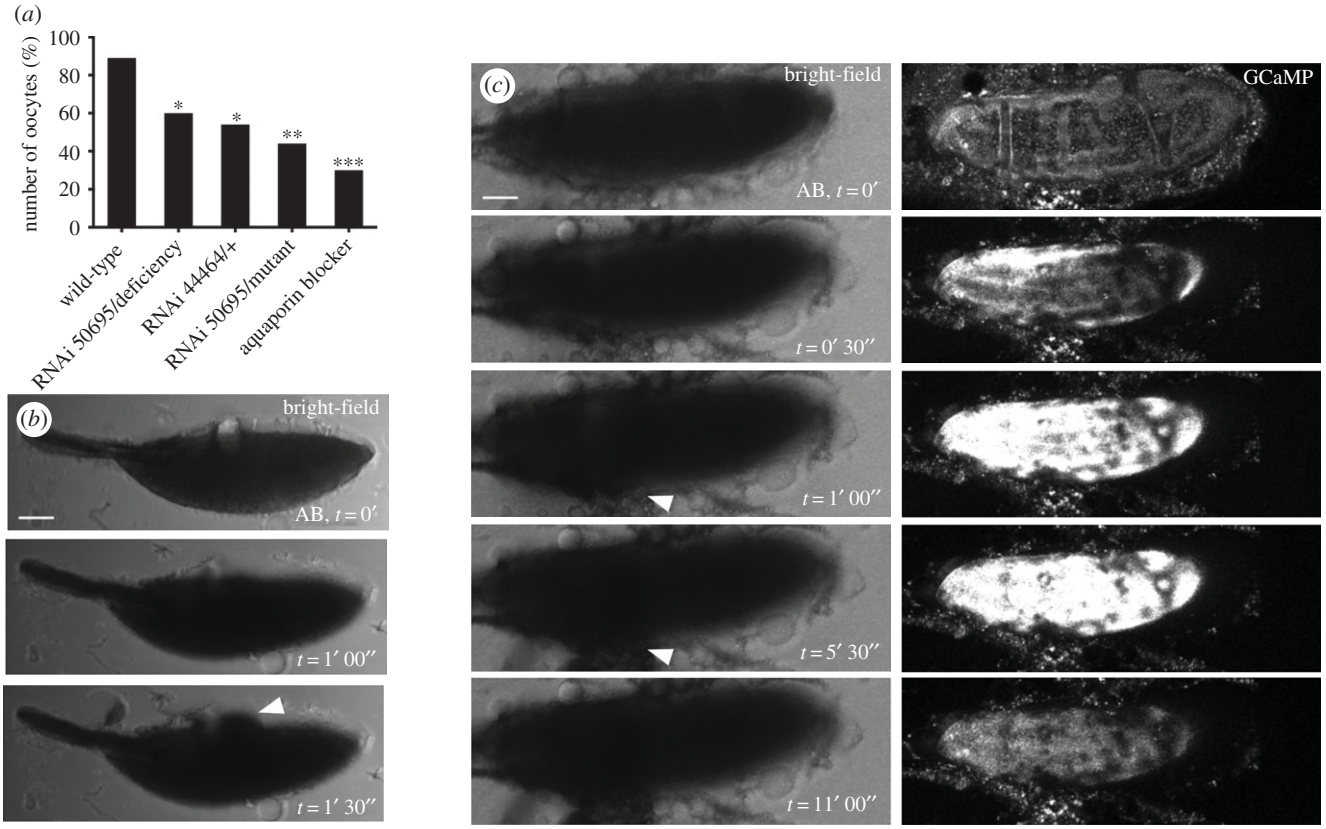

Figure 3. Water homeostasis is required for egg activation. (*a*) The data show the presence of a single full calcium wave in aquaporin depleted backgrounds upon the addition of AB. Aquaporin depletion was achieved through knockdown using BL50695 (germline) and BL44464 (germline and somatic) RNAi, deficiency (Df(2R)BSC160/Cyo), *prip* mutant (y1; P{SUPor-P}PripKG08662) and the broad, non-specific, aquaporin channel antagonist copper sulfate. Upon the addition of AB, the number of oocytes with the calcium wave significantly decreased to 50% in the germline knockdown over the deficiency ($n = 25$, $p < 0.05$) or mutant ($n = 18$, $p < 0.001$). A similar significant decrease was also observed with only one copy knock-down of both somatic and germline Prip (BL44464) ($n = 13$, $p < 0.05$). Addition of 2 mm copper sulfate results in a significant decrease of waves to approximately 30% ($n = 44$, $p < 0.001$). The number of burst phenotypes was quantified across experimental conditions and the mean value was 50% bursts, compared to 3% bursts in the wild-type. (*b*) Bright-field time series of mature egg chamber in an aquaporin depleted background (RNAi 50695/deficiency). Upon addition of AB, the oocyte bursts and the cytoplasm is visible leaking out within 1 min and 30 s (white arrowhead) ($n = 72$). Scale bar 60 µm. Maximum projection 40 µm. (*c*) Time series of *ex vivo* mature egg chamber expressing *UAS-myrGCaMP5* and two copies of *ripped-pocket* RNAi following the addition of AB. The cortical increase appears within 30 s of the addition of AB, which is followed by the oocyte burst and cytoplasm leaking out in 74% of egg chambers (white arrowhead). The dark spots represent excess tissue and oil droplets. Scale bar 60 µm. Maximum projection 40 µm.

AQP channel antagonist) into AB, we do not observe a calcium wave (figure 3*a*).

There is only one AQP channel, Prip, that is known to be expressed in the *Drosophila* ovarian tissue (*Drosophila* Fly Atlas). To investigate the role of Prip at egg activation, we used knock-down tools in heterozygous deficiency or mutant backgrounds since the homozygous mutant was lethal. Upon the addition of AB, eggs swell as normal, however, the number of oocytes showing a calcium wave significantly decreased in egg chambers expressing various AQP-deficient backgrounds (figure 3*a*). We further investigated the effect of Prip disruption by observing the time series of *ex vivo* activated eggs and found that half of these eggs rupture and leak cytoplasm shortly after the addition of AB (figure 3*b*). Interestingly, some eggs were still able to initiate and propagate a calcium wave despite rupturing. These data are strongly suggestive of a subsequent requirement for Prip in mediating water homeostasis at egg activation.

Similar effects were observed in egg chambers expressing reduced levels of *ripped-pocket (rpk)*, a member of the mechanosensitive channels family DEG/ENaC known to interact with F-actin be involved in transducing changes in osmotic pressure [34–37]. When activated, these egg chambers show a cortical calcium increase, rupture of the plasma membrane and leaking of the cytoplasm (figure 3*c*). This phenotype is similar when eggs are exposed to low-osmolarity solutions (figure 2*a*′), suggesting that *rpk* is required to mediate water entry. Together, these data suggest that one of the roles of AQP and DEG/ENaC channels is to coordinate optimal swelling and water homeostasis at egg activation.

2.5. External calcium is not required for initiation and propagation of the calcium wave

In many animals, external and/or internal calcium is required for the calcium rise at egg activation [4]. To investigate the source of calcium at *Drosophila* egg activation, *ex vivo* mature egg chambers were treated with AB containing the calcium chelator BAPTA. These eggs exhibited typical swelling and a full-calcium wave (figure 4*a*), suggesting that external calcium from the surrounding solution is not required. To further validate this experiment, we depleted internal calcium by pre-incubating egg chambers with membrane-permeable BAPTA-AM (with solubilizing agent PF-127). Following the addition of AB, we observed a

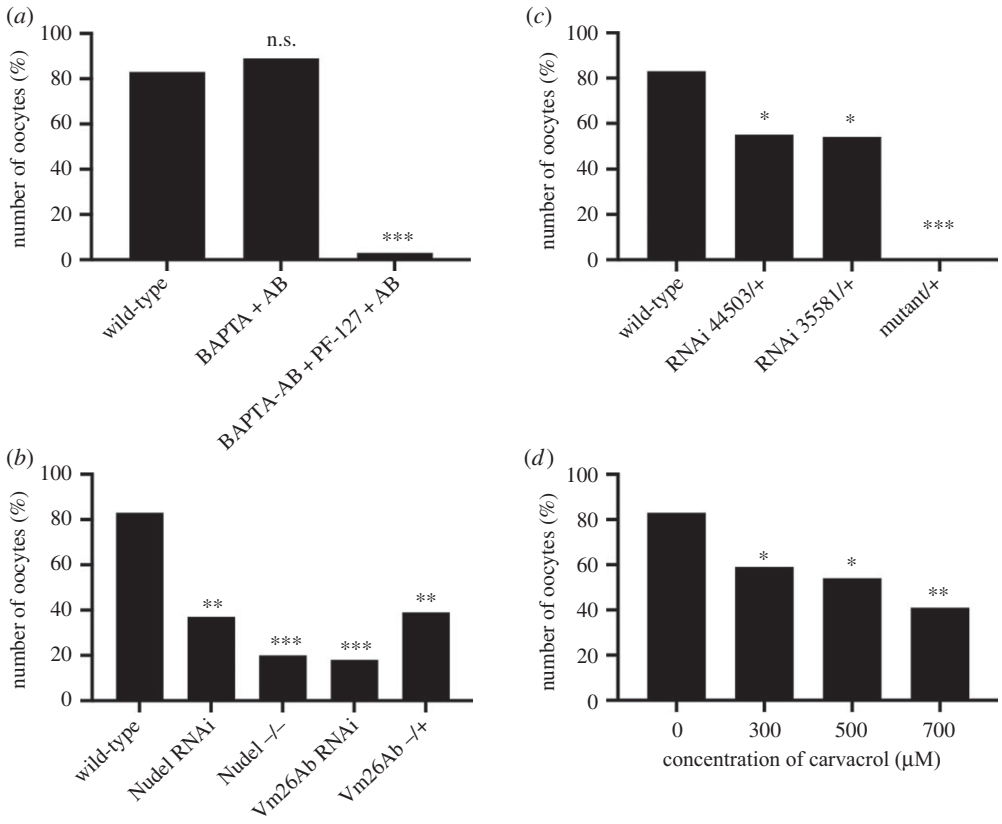

Figure 4. Internal calcium and Trpm channel are required for the calcium wave. (*a*) The graph shows the presence of the calcium wave in external or internal calcium-depleted backgrounds. Depletion of external calcium was achieved through the addition of calcium chelator BAPTA in AB and showed no significant difference in the number of oocytes with the calcium wave ($n = 19$ and $n = 57$). Depletion of calcium in the egg chamber was achieved through incubation with BAPTA-AM and PF-127 prior to the addition of AB and resulted in a significant decrease in the number of calcium waves ($n = 34$, $p < 0.001$). Data were statistically analysed using Fisher's exact test. (*b*) The graph shows the proportion of single full calcium waves in mature oocytes with genetic depletion of vitelline membrane proteins (essential for production and integrity) following the addition of AB. Nudel depletion was achieved through knockdown using BL65142 (somatic and germline) and through homozygous mutation (*Vm26Ab[QJ42] cn*[1] *bw*[1]*/CyO, l(2)DTS513*[1]). Upon the addition of AB, the number of oocytes displaying a calcium wave significantly decreased in both the knockdown ($n = 19$, $p < 0.01$) and knockout ($n = 48$, $p < 0.001$). Sv23 (Vm26Ab) depletion was achieved through knockdown using BL65022 (somatic and germline) and through heterozygous mutation (*mwh*[1] *ndl*[7] *red*[1] *e*[1]*/TM1*) as homozygous mutants were not viable. Again, upon the addition of AB, the number of oocytes displaying a calcium wave significantly decreased in both the knockdown ($n = 32$, $p < 0.05$) and heterozygous mutant ($n = 38$, $p < 0.01$). Data were statistically analysed using Fisher's exact test. (*c–d*) The graphs show the presence of the calcium waves following swelling in Trpm depleted backgrounds. Trpm depletion was achieved through knockdown using BL44503 (somatic and germline) and BL35581 (germline) RNAi, *trpm* mutant (y1 w67c23; P{EPgy2}TrpmEY01618/CyO) (*c*) and (*d*) the broad Trpm blocker carvacrol. Upon the addition of AB (*c*), the number of the oocytes with the calcium wave significantly decreased with only one copy knockdown of both somatic and germline Trpm (BL44503) ($n = 96$, $p < 0.01$) and germline only (BL35581) ($n = 35$, $p < 0.05$). A significant decrease in the number of the calcium waves was also observed in Trpm mutant background ($n = 14$, $p < 0.001$). (*d*) A significant decrease in the number of the calcium waves was also observed with the addition of AB with the broad Trpm blocker carvacrol in a concentration-dependent manner of 300 µm ($n = 27$, $p < 0.05$), 500 µM ($n = 24$, $p < 0.05$) and 700 µm ($n = 24$, $p < 0.01$). Data were statistically analysed using Fisher's exact test.

significantly reduced number of calcium events (figure 4*a*). Together, these findings point towards the source of calcium residing within the mature egg chamber.

There are several potential internal calcium sources in the mature egg chamber, including the perivitelline space surrounding the mature oocyte [22]. The perivitelline space has been shown to contain different ions, including calcium in the early *Drosophila* embryo [38]. While it remains technically not possible to extract this fluid from the mature egg chamber due to the dehydrated morphology, we tested the role of the perivitelline space through genetic disruption of the vitelline membrane. We used RNAi and mutations to knockdown the protease Nudel and the vitelline membrane gene Vm26Ab (which encodes Sv23), both of which are known to be required for production and integrity of the vitelline membrane [39,40]. Following the addition of AB, the egg chambers showed a significant decrease in the number of calcium waves at egg activation (figure 4*b*). Together these data support a model in which the perivitelline space acts as a store of calcium prior to the calcium wave at egg activation, as disruption of the vitelline membrane prevents calcium waves from occurring following the addition of AB.

One candidate that would mediate calcium entry from the perivitelline space into the oocyte is the mechanosensitive channel Trpm. This transmembrane channel was recently shown to be required for the entry of calcium into the oocyte [25]. To further this conclusion, we used similar approaches with different experimental specifications. Our analysis used a transgenic line from Berkeley *Drosophila* Genome Project, which is a transposon P-element insertion in the 39th splice site which results in an imprecise deletion of three exons of Trpm [41,42]. Upon the addition of AB, these mature egg chambers swelled as expected, but failed to initiate a calcium increase (figure 4*c*). We also used two RNAi lines in heterozygous egg chambers which resulted in a significant reduction in calcium waves (figure 4*c*).

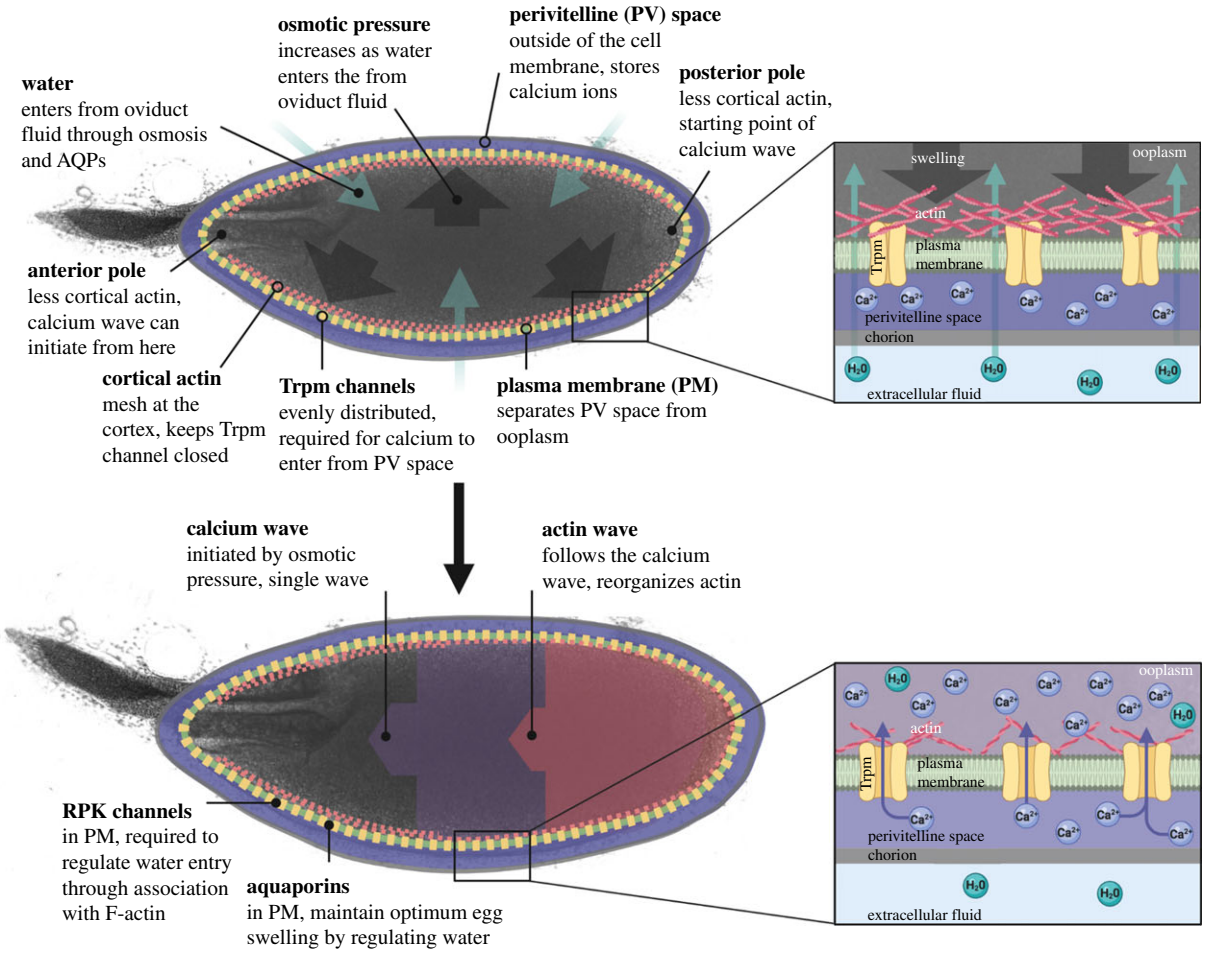

Figure 5. Model of *Drosophila* egg activation. Essential components and processes of *Drosophila* egg activation are outlined in the panels. A comprehensive description of the model is included in the discussion. Created with BioRender.com.

Together, this suggests that there could be a concentration-dependent response of Trpm. To test this hypothesis, egg chambers wild-type for Trpm were incubated with different concentrations of carvacrol, a broad Trpm inhibitor [43]. The addition of AB with carvacrol resulted in a significant decrease in the number of eggs with a calcium wave at a range of concentrations (figure 4*d*). These data support the findings that Trpm is involved in regulating the entry of calcium into the mature oocyte at egg activation. Since Trpm channels are located in the plasma membrane [25], it is likely that their role is to allow calcium from the perivitelline space to enter the oocyte at activation.

3. Discussion

3.1. Model of *Drosophila* egg activation

In summary, our *ex vivo* data show that the calcium wave and characteristic downstream events associated with egg activation are initiated by osmotic pressure generated by the uptake of external fluid. We show that AQP and DEG/ENaC channels are required for mediating water homeostasis to withstand the rise in osmotic pressure during egg activation. We present complementary evidence that the Trpm channel is required for the influx of calcium, which we show is not supplied from a source outside of the egg chamber.

Together with previous work, our data support the following model of *Drosophila* egg activation (figure 5): (i) at ovulation, the meiotically arrested mature oocyte passes into the lateral and then common oviduct; (ii) the mature oocyte then takes up fluid due to the difference in osmolarity between the oviduct fluid and the ooplasm; (iii) the increase in volume results in tension at the plasma membrane and dispersion of the cortical actin; (iv) volume increase is mediated by association of RPK with cortical actin; (v) decreased density of cortical actin at the poles, prior to dispersion, primes these regions for calcium entry; (vi) calcium likely enters the egg from the perivitelline space through the mechanosensitive Trpm channels in the plasma membrane; (vii) starting at the posterior pole, further increase in intracellular calcium may be relayed across the oocyte by the opening of the neighbouring Trpm channels via the dispersion of the cortical actin cytoskeleton at the lateral sides, in addition to IP3- and PLC-mediated calcium propagation [6,24]; (viii) the calcium wave is then followed by an F-actin wavefront, which ensures the reorganization of the actin cytoskeleton; (ix) intracellular calcium returns to basal levels, likely through channels that transport calcium back into the perivitelline space or intracellular stores. Collectively, the single calcium wave prepares the oocyte for pronuclear apposition and embryogenesis [44].

Osmotic pressure is a common mechanism for a volume increase and a rise in intracellular calcium levels, exemplified by intestinal epithelial cells, human osteoblast-like cells, rat

astrocytes and cancer cell lines [45–48]. It is hypothesized that cells sense an increase in cell volume via intracellular solute, membrane-bound, and/or cytoskeletal sensors [49]. The application of osmotic pressure seems to be a conserved initiation cue for egg activation in insects. Previous work has shown that the immersion of the oviposited mature oocytes of the yellow fever mosquito into water can resume oocyte development [50]. Similarly, for oocytes of the turnip sawfly and the malaria vector mosquito, egg activation can be initiated by placing the oocytes into water [16,17].

Drosophila is currently the only example of an insect in which the mature oocytes have been shown to exhibit an increase in intracellular calcium in response to the addition of hypotonic solution [5,6]. Our results presented here show that osmotic pressure acts as an initiation cue of the calcium wave at *Drosophila* egg activation.

3.2. AQP and RPK requirement in water homeostasis

It is essential to regulate cellular volume in response to changes in osmotic pressure. This is often achieved by AQPs, a conserved channel known to control the influx and efflux of water during cellular processes, including cell migration, neuroexcitation and epithelial fluid transport [32]. In *Drosophila*, our findings show the AQP Prip is required to maintain an optimal volume change at egg activation. In a *Prip*-depleted background, we observed eggs initially swelling but rupturing shortly after. Interestingly, RNAi depletion and CRISPR deletion showed that Prip (*CG7777*) is not required for female fertility [51] suggesting that a compensatory mechanism acts *in vivo* to maintain water homeostasis and prevent egg rupture.

In addition, we show that the depletion of the DEG/ENaC channel, *rpk*, also results in oocytes rupturing when activated. We propose that RPK mediates optimal swelling through interactions with the cortical actin cytoskeleton, which we have previously shown to be re-organized at egg activation [27]. This hypothesis is supported by (i) co-immunoprecipitation studies in MDCK cells in which DEG/ENaC channels bind F-actin via the COOH terminus of α-ENaC and (ii) mechanical pressure experiments that activate DEG/ENaC channels resulting in the stiffening of the cortical actin in vascular endothelial cells [37,52]. We therefore propose that RPK is stabilizing the cortical actin to withstand the increase in volume at activation.

3.3. Role of osmotic pressure and TRP channels at egg activation

Recent work on germline knockout mutants and RNAi in *Drosophila* has established the requirement of mechanosensitive Trpm channels in mediating the calcium influx at egg activation [25]. We corroborate this requirement using different mutants, RNAi and pharmacological disruption. Our data support a model in which osmotic pressure generates tension in the plasma membrane and the cortical actin resulting in the opening of Trpm channels and subsequent calcium entry. Interestingly, the mammalian homologue TRPM3 is also activated in HEK293 cells by the application of a hypotonic solution, resulting in an intracellular calcium increase [53]. Similarly, in mammalian sensory neurons, TRPV4 and TRPV1 respond to changes in osmotic pressure [54–57].

Calcium entry mediated by TRP channels appears to be a conserved mechanism in the eggs of many animals. This was first shown in *Xenopus laevis* oocytes where a mechanical stimulus resulted in the opening of TRPC1 [58]. More recently, mouse oocytes have been shown to require TRPV3 for the calcium intracellular increase and were affected by overexpression and the application of 2-APB [59]. In addition, TRPM7 was also shown to be essential for the calcium influx at mouse egg activation [60]. Finally, in *Caenorhabditis elegans* loss of the TRP3 channel resulted in a failure to show a calcium rise at egg activation [61]. Taken together these examples highlight a conserved role of TRP channels in mediating successful egg activation through calcium entry.

3.4. The source of calcium at *Drosophila* egg activation

Calcium waves at egg activation can be mediated by intracellular and/or external calcium sources [4]. In *Drosophila*, Trpm regulates calcium entry across the plasma membrane suggesting that the calcium source is external to the oocyte. Paradoxically, we also show that external calcium is not required for a wild-type calcium wave. We argue that these data are compatible and point to the perivitelline space, situated between the oocyte plasma membrane and the vitelline membrane, as a calcium store. The composition of the perivitelline space in the egg chamber is currently unknown. However, in the early embryo, it has been shown to contain many ions, including calcium [38]. Our work supports a model where the perivitelline space is pre-loaded with calcium during oogenesis which enters through Trpm channels when the egg swells. This model is supported by our data showing that the injection of oil (devoid of calcium) is sufficient to induce a calcium rise in the oocyte and mutant analysis of the vitelline membrane. It is also possible that physical manipulation or altering the integrity of the vitelline membrane may affect receptors or regulator proteins in the plasma membrane which could account for the decrease in calcium waves.

3.5. The *Drosophila* calcium wave is an example of a 'slow' calcium wave

While calcium waves can be classified by the source of ions, they can alternatively be compared based on how fast they propagate [62]. In most animals, calcium waves at egg activation are classified as fast, travelling at approximately 10–30 $\mu m\ s^{-1}$ [63]. However, some wave(s) propagate at approximately 0.2–2 $\mu m\ s^{-1}$ and are classified as slow [62]. This includes calcium influx at egg activation in maize eggs which propagates at 1.13 $\mu m\ s^{-1}$ and interestingly, requires mechanosensitive channels [64–66]. This is very similar to observations in *Drosophila*, where mechanosensitive channels and the actin cytoskeleton are required for a slow wave that propagates at approximately 1.5 $\mu m\ s^{-1}$. In fact, the general mechanism for a slow calcium wave [60] is strikingly similar to what we propose is occurring at *Drosophila* egg activation.

Overall, aspects of the calcium wave, and more broadly egg activation, in *Drosophila* appear to be conserved with a variety of other organisms. Further analysis in flies will likely show even more similarities and inform our overall understanding of egg activation in all species.

4. Material and methods

4.1. Fly stocks

The following fly stocks were used: *UASt-myristoylated(myr)-GCaMP5*); *matα-GAL4::VP16* (BL7063) and *UASp-GCaMP3* [6]; *tub-GAL4VP16* (Siegfried Roth); *jupiter-mCherry* (Paul Conduit); *me31B::GFP* [67]; *Nudel RNAi* (P{y[+ t7.7] v[+ t1.8] = TRiP.HMC03171}attP40, BL65142); *Nudel mutant* (mwh[1] ndl[7] red[1] e[1]/TM1, BL9036); *Vm26Ab RNAi* (P{y[+ t7.7] v[+ t1.8] = TRiP.HMC05896}attP40, BL65022); *Vm26Ab mutant* (Vm26Ab[QJ42] cn[1] bw[1]/CyO, l(2)DTS513[1], BL5118); *ripped-pocket RNAi* (P{TRiP.HMS01973}attP40, BL39053); *trpm mutant* (P{EPgy2}TrpmEY01618/CyO, BL15365); *trpm RNAi* (BL35581 and BL44503); *prip mutant* (P{SUPor-P}PripKG08662, BL14750); *prip RNAi* (P{TRiP.GLC01619}attP2, BL44464); *prip RNAi* (P{TRiP.HMC03097}attP40, BL50695); deficiency (for *prip*) (*Df(2R)BSC160/CyO*, BL9595). Stocks were raised on standard cornmeal-agar medium at 21°C or 25°C. For dissection of mature oocytes, mated females were fattened on yeast for 48 h at 25°C.

4.2. Reagents

BAPTA (Sigma-Aldrich) was used at a final concentration of 10 µM; BAPTA-AM + PF-127 (Sigma-Aldrich) was used at a final concentration of 30 µM; carvacrol (Sigma-Aldrich) used at 300–700 µm; copper sulfate (Sigma-Aldrich) was used at a final concentration of 2 mm. Standard preparation protocols were used as according to Sigma-Aldrich.

AB, 260 mOsm, containing 3.3 mm NaH_2PO_4, 16.6 mm KH_2PO_4, 10 mm NaCl, 50 mm KCl, 5% polyethylene glycol 8000, 2 mm $CaCl_2$, brought to pH 6.4 with a 1 : 5 ratio of NaOH : KOH [15]; Gibco Schneider's *Drosophila* Medium, approximately 360 mOsm, a standard *Drosophila* culture medium that does not initiate egg activation (Thermo Fisher); Series95 halocarbon oil (KMZ Chemicals); EZ-Squeeze tube 125 µm (Cooper Surgical). For osmolarity experiments, sucrose (Sigma-Aldrich) was directly dissolved into distilled water and the osmolarity was measured using an osmometer (Löser).

4.3. Preparation of mature oocyte for live imaging

Mature oocytes were dissected from the ovaries from fattened flies using a probe and fine forceps [68]. Dissected oocytes were placed in series 95 halocarbon oil (KMZ Chemicals) on 22 × 40 coverslips, aligned parallel to each other to maximize the acquisition area for imaging, left to settle for 10 min, and incubated in solution *ex vivo* [68].

4.4. Imaging

Time series were acquired with an inverted Leica SP5, under 20 × 0.7NA immersion objective. The Z-stacks were acquired at 2 µm steps from the first visible plane to 40 µm deep. The Z-stacks were presented as maximum projections of the 40 µm unless stated otherwise.

4.5. Oil injection

Preparation for microinjection was carried out with a Femtotips II microinjection needle (Eppendorf) and a gas pressure injection system were used to inject oil into the Stage 14 egg chambers [31]. Imaging was performed simultaneously with injection on a DeltaVision wide-field microscope (Applied Precision) using a 20 × 0.75 NA numerical aperture.

4.6. Quantifications and analysis

The calcium wave data were analysed statistically using Fisher's exact test with p-values ($p < 0.05$ considered significantly different) [6]. The spindle dimensions were quantified and statistically analysed using an unpaired t-test with $p < 0.05$ values showing significant difference. The number of asterisks represents the p-value: $*p \leq 0.05$, $**p \leq 0.01$, $***p \leq 0.001$.

Data accessibility. This article has no additional data.

Competing interests. We declare we have no competing interests.

Funding. Funding received from the University of Cambridge ISSF grant no. 097814 (to T.T.W.), Department of Zoology Balfour Studentship (to A.H.Y.A.), BBSRC DTP studentship (to B.W.W. and E.L.W.) and Sir Isaac Newton Trust Research Grant (Ref. 18.07ii(c)).

Acknowledgements. We are grateful to Richard Parton for experimental and technical advice; Mariana Wolfner, Matthias Landgraf, Howard Baylis, José Casal, Peter Lawrence for feedback, discussions and advice; Richard York-Weaving for feedback on the manuscript; the Zoology Imaging Facility and Matt Wayland for assistance with microscopy; Siegfried Roth, Paul Conduit and Mariana Wolfner for fly stocks.

References

1. Whitaker M. 2006 Calcium at fertilization and in early development. *Physiol. Rev.* **86**, 25–88. (doi:10.1152/physrev.00023.2005)
2. Horner VL, Wolfner MF. 2008 Transitioning from egg to embryo: triggers and mechanisms of egg activation. *Dev. Dyn.* **237**, 527–544. (doi:10.1002/dvdy.21454)
3. Swann K, Lai FA. 2016 Egg activation at fertilization by a soluble sperm protein. *Physiol. Rev.* **96**, 127–149. (doi:10.1152/physrev.00012.2015)
4. Stricker SA. 1999 Comparative biology of calcium signaling during fertilization and egg activation in animals. *Dev. Biol.* **211**, 157–176. (doi:10.1006/dbio.1999.9340)
5. York-Andersen AH, Parton RM, Bi CJ, Bromley CL, Davis I, Weil TT. 2015 A single and rapid calcium wave at egg activation in *Drosophila*. *Biol. Open* **4**, 553–560. (doi:10.1242/bio.201411296)
6. Kaneuchi T, Sartain CV, Takeo S, Horner VL, Buehner NA, Aigaki T, Wolfner MF. 2015 Calcium waves occur as *Drosophila* oocytes activate. *Proc. Natl Acad. Sci. USA* **112**, 791–796. (doi:10.1073/pnas.1420589112)
7. Parrington J, Davis LC, Galione A, Wessel G. 2007 Flipping the switch: how a sperm activates the egg at fertilization. *Dev. Dyn.* **236**, 2027–2038. (doi:10.1002/dvdy.21255)
8. Horner VL, Wolfner MF. 2008 Mechanical stimulation by osmotic and hydrostatic pressure activates *Drosophila* oocytes *in vitro* in a calcium-dependent manner. *Dev. Biol.* **316**, 100–109. (doi:10.1016/j.ydbio.2008.01.014)
9. Kishimoto T. 1998 Cell cycle arrest and release in starfish oocytes and eggs. *Semin. Cell Dev. Biol.* **9**, 549–557. (doi:10.1006/scdb.1998.0249)

10. Harada K, Oita E, Chiba K. 2003 Metaphase I arrest of starfish oocytes induced via the MAP kinase pathway is released by an increase of intracellular pH. *Development* **130**, 4581–4586. (doi:10.1242/dev.00649)
11. Lindsay LL, Hertzler PL, Clark WH. 1992 Extracellular Mg^{2+} induces an intracellular Ca^{2+} wave during oocyte activation in the marine shrimp *Sicyonia ingentis*. *Dev. Biol.* **152**, 94–102. (doi:10.1016/0012-1606(92)90159-e)
12. Went DF. 1982 Egg activation and parthenogenetic reproduction in insects. *Biol. Rev.* **57**, 319–344. (doi:10.1111/j.1469-185x.1982.tb00371.x)
13. Went DF, Krause G. 1973 Normal development of mechanically activated, unlaid eggs of an endoparasitic hymenopteran. *Nature* **244**, 454–455. (doi:10.1038/244454a0)
14. Went DF, Krause G. 1974 Alteration of egg architecture and egg activation in an endoparasitic hymenopteran as a result of natural or imitated oviposition. *Wilhelm Roux' Archiv Für Entwicklungsmechanik Der. Org.* **175**, 173–184. (doi:10.1007/bf00582090)
15. Mahowald AP, Goralski TJ, Caulton JH. 1983 *In vitro* activation of *Drosophila* eggs. *Dev. Biol.* **98**, 437–445. (doi:10.1016/0012-1606(83)90373-1)
16. Yamamoto DS, Hatakeyama M, Matsuoka H. 2013 Artificial activation of mature unfertilized eggs in the malaria vector mosquito, *Anopheles stephensi* (Diptera, Culicidae). *J Exp Biol* **216**, 2960–2966. (doi:10.1242/jeb.084293)
17. Oishi K, Sawa M, Hatakeyama M, Kageyama Y. 1993 Genetics and biology of the sawfly, *Athalia rosae* (Hymenoptera). *Genetica* **88**, 119–127. (doi:10.1007/bf02424468)
18. Tojo K, Machida R. 1998 Early embryonic development of the mayfly *Ephemera japonica* McLachlan (Insecta: Ephemeroptera, Ephemeridae). *J. Morphol.* **238**, 327–335. (doi:10.1002/(sici)1097-4687(199812)238:3<327::aid-jmor4>3.0.co;2-j)
19. Li J. 1994 Egg chorion tanning in *Aedes aegypti* mosquito. *Comp. Biochem. Physiol. Part Physiol.* **109**, 835–843. (doi:10.1016/0300-9629(94)90231-3)
20. Li JS, Li J. 2006 Major chorion proteins and their crosslinking during chorion hardening in *Aedes aegypti* mosquitoes. *Insect Biochem. Molec* **36**, 954–964. (doi:10.1016/j.ibmb.2006.09.006)
21. Doane WW. 1960 Completion of meiosis in uninseminated eggs of *Drosophila melanogaster*. *Science* **132**, 677–678. (doi:10.1126/science.132.3428.677)
22. Sartain CV, Wolfner MF. 2013 Calcium and egg activation in *Drosophila*. *Cell Calcium* **53**, 10–15. (doi:10.1016/j.ceca.2012.11.008)
23. Lin H, Spradling AC. 1993 Germline stem cell division and egg chamber development in transplanted *Drosophila* Germaria. *Dev. Biol.* **159**, 140–152. (doi:10.1006/dbio.1993.1228)
24. Hu Q, Vélez-Avilés AN, Wolfner MF. 2020 *Drosophila* Plc21C is involved in calcium wave propagation during egg activation. *Micropublication Biol.* **2020**, 235. (doi:10.17912/micropub.biology.000235)
25. Hu Q, Wolfner MF. 2019 The *Drosophila* Trpm channel mediates calcium influx during egg activation. *Proc. Natl Acad. Sci. USA* **116**, 18 994–19 000. (doi:10.1073/pnas.1906967116)
26. Hu Q, Wolfner MF. 2020 Regulation of Trpm activation and calcium wave initiation during *Drosophila* egg activation. *Mol. Reprod. Dev.* **87**, 880–886. (doi:10.1002/mrd.23403)
27. York-Andersen AH, Hu Q, Wood BW, Wolfner MF, Weil TT. 2020 A calcium-mediated actin redistribution at egg activation in *Drosophila*. *Mol. Reprod. Dev.* **87**, 293–304. (doi:10.1002/mrd.23311)
28. Endow SA, Komma DJ. 1997 Spindle dynamics during meiosis in *Drosophila* oocytes. *J. Cell Biol.* **137**, 1321–1336. (doi:10.1083/jcb.137.6.1321)
29. Page AW, Orr-Weaver TL. 1997 Activation of the meiotic divisions in *Drosophila* oocytes. *Dev. Biol.* **183**, 195–207. (doi:10.1006/dbio.1997.8506)
30. Heifetz Y, Yu J, Wolfner MF. 2001 Ovulation triggers activation of *Drosophila* oocytes. *Dev. Biol.* **234**, 416–424. (doi:10.1006/dbio.2001.0246)
31. Weil TT *et al.* 2012 *Drosophila* patterning is established by differential association of mRNAs with P bodies. *Nat. Cell Biol.* **14**, 1305–1313. (doi:10.1038/ncb2627)
32. Verkman AS. 2011 Aquaporins at a glance. *J. Cell Sci.* **124**, 2107–2112. (doi:10.1242/jcs.079467)
33. Verkman AS, Anderson MO, Papadopoulos MC. 2014 Aquaporins: important but elusive drug targets. *Nat. Rev. Drug Discov.* **13**, 259–277. (doi:10.1038/nrd4226)
34. Chalfie M, Wolinsky E. 1990 The identification and suppression of inherited neurodegeneration in *Caenorhabditis elegans*. *Nature* **345**, 410–416. (doi:10.1038/345410a0)
35. Driscoll M, Chalfie M. 1991 The mec-4 gene is a member of a family of *Caenorhabditis elegans* genes that can mutate to induce neuronal degeneration. *Nature* **349**, 588–593. (doi:10.1038/349588a0)
36. García-Añoveros J, Ma C, Chalfie M. 1995 Regulation of *Caenorhabditis elegans* degenerin proteins by a putative extracellular domain. *Curr. Biol.* **5**, 441–448. (doi:10.1016/s0960-9822(95)00085-6)
37. Mazzochi C, Bubien JK, Smith PR, Benos DJ. 2006 The carboxyl terminus of the α-subunit of the amiloride-sensitive epithelial sodium channel binds to F-actin. *J. Biol. Chem.* **281**, 6528–6538. (doi:10.1074/jbc.m509386200)
38. van der Meer JM, Jaffe LF. 1983 Elemental composition of the perivitelline fluid in early *Drosophila* embryos. *Dev Biol* **95**, 249–252. (doi:10.1016/0012-1606(83)90025-8)
39. LeMosy EK, Hashimoto C. 2000 The Nudel protease of *Drosophila* is required for eggshell biogenesis in addition to embryonic patterning. *Dev. Biol.* **217**, 352–361. (doi:10.1006/dbio.1999.9562)
40. Manogaran A, Waring GL. 2004 The N-terminal pro domain of sV23 is essential for the assembly of a functional vitelline membrane network in *Drosophila*. *Dev. Biol.* **270**, 261–271. (doi:10.1016/j.ydbio.2004.02.009)
41. Bellen HJ *et al.* 2004 The BDGP gene disruption project single transposon insertions associated with 40 of *Drosophila* genes. *Genetics* **167**, 761–781. (doi:10.1534/genetics.104.026427)
42. Hofmann T, Chubanov V, Chen X, Dietz AS, Gudermann T, Montell C. 2010 *Drosophila* TRPM channel is essential for the control of extracellular magnesium levels. *PLoS ONE* **5**, e10519. (doi:10.1371/journal.pone.0010519)
43. Chubanov V, Schäfer S, Ferioli S, Gudermann T. 2014 Natural and synthetic modulators of the TRPM7 channel. *Cells* **3**, 1089–1101. (doi:10.3390/cells3041089)
44. Callaini G, Riparbelli MG. 1996 Fertilization in *Drosophila melanogaster*: centrosome inheritance and organization of the first mitotic spindle. *Dev. Biol.* **76**, 199–208. (doi:10.1006/dbio.1996.0127)
45. O'Connor E, Kimelberg H. 1993 Role of calcium in astrocyte volume regulation and in the release of ions and amino acids. *J. Neurosci.* **13**, 2638–2650. (doi:10.1523/jneurosci.13-06-02638.1993)
46. MacLeod RJ, Hamilton JR. 1999 Increases in intracellular pH and Ca^{2+} are essential for K^+ channel activation after modest 'physiological' swelling in villus epithelial cells. *J. Membr. Biol.* **172**, 47–58. (doi:10.1007/s002329900582)
47. Weskamp M, Seidl W, Grissmer S. 2000 Characterization of the increase in $[Ca^{2+}]_i$ during hypotonic shock and the involvement of Ca^{2+}-activated K^+ channels in the regulatory volume decrease in human osteoblast-like cells. *J. Membr. Biol.* **178**, 11–20. (doi:10.1007/s002320010010)
48. Shen M, Chou C, Browning JA, Wilkins RJ, Ellory JC. 2001 Human cervical cancer cells use Ca^{2+} signalling, protein tyrosine phosphorylation and MAP kinase in regulatory volume decrease. *J. Physiol.* **537**, 347–362. (doi:10.1111/j.1469-7793.2001.00347.x)
49. Kültz D, Burg MB. 1998 Intracellular signaling in response to osmotic stress. *Contrib. Nephrol.* **123**, 94–109. (doi:10.1159/000059923)
50. Kliewer JW. 1961 Weight and hatchability of *Aedes aegypti* eggs (Diptera: Culicidae)1. *Ann Entomol Soc Am* **54**, 912–917. (doi:10.1093/aesa/54.6.912)
51. Avilés-Pagán EE, Kang ASW, Orr-Weaver TL. 2020 Identification of new regulators of the oocyte-to-embryo transition in *Drosophila*. *G3 Genes|Genomes|Genetics* **10**, 2988–2998. (doi:10.1534/g3.120.401415)
52. Kusche-Vihrog K, Urbanova K, Blanqué A, Wilhelmi M, Schillers H, Kliche K, Pavenstädt H, Brand E, Oberleithner H. 2011 C-Reactive protein makes human endothelium stiff and tight. *Hypertension* **57**, 231–237. (doi:10.1161/hypertensionaha.110.163444)
53. Grimm C, Kraft R, Sauerbruch S, Schultz G, Harteneck C. 2003 Molecular and functional characterization of the melastatin-related cation channel TRPM3. *J. Biol. Chem.* **278**, 21 493–21 501. (doi:10.1074/jbc.m300945200)
54. Liedtke W, Choe Y, Martí-Renom MA, Bell AM, Denis CS, AndrejŠali HA, Friedman JM, Heller S. 2000 Vanilloid receptor-related osmotically activated channel (VR-OAC), a candidate vertebrate osmoreceptor. *Cell* **103**, 525–535. (doi:10.1016/s0092-8674(00)00143-4)

55. Strotmann R, Harteneck C, Nunnenmacher K, Schultz G, Plant TD. 2000 OTRPC4, a nonselective cation channel that confers sensitivity to extracellular osmolarity. *Nat. Cell Biol.* **2**, 695–702. (doi:10.1038/35036318)
56. Naeini RS, Witty M-F, Séguéla P, Bourque CW. 2006 An N-terminal variant of Trpv1 channel is required for osmosensory transduction. *Nat. Neurosci.* **9**, 93–98. (doi:10.1038/nn1614)
57. Ciura S, Liedtke W, Bourque CW. 2011 Hypertonicity sensing in organum vasculosum lamina terminalis neurons: a mechanical process involving TRPV1 but not TRPV4. *J. Neurosci.* **31**, 14 669–14 676. (doi:10.1523/jneurosci.1420-11.2011)
58. Methfessel C, Witzemann V, Takahashi T, Mishina M, Numa S, Sakmann B. 1986 Patch clamp measurements on *Xenopus laevis* oocytes: currents through endogenous channels and implanted acetylcholine receptor and sodium channels. *Pflügers Archiv.* **407**, 577–588. (doi:10.1007/bf00582635)
59. Lee HC, Yoon S-Y, Lykke-Hartmann K, Fissore RA, Carvacho I. 2016 TRPV3 channels mediate Ca^{2+} influx induced by 2-APB in mouse eggs. *Cell Calcium* **59**, 21–31. (doi:10.1016/j.ceca.2015.12.001)
60. Carvacho I, Ardestani G, Lee HC, McGarvey K, Fissore RA, Lykke-Hartmann K. 2016 TRPM7-like channels are functionally expressed in oocytes and modulate post-fertilization embryo development in mouse. *Sci. Rep-UK* **6**, 34236. (doi:10.1038/srep34236)
61. Takayama J, Onami S. 2016 The sperm TRP-3 channel mediates the onset of a Ca^{2+} wave in the fertilized *C. elegans* oocyte. *Cell Reports* **15**, 625–637. (doi:10.1016/j.celrep.2016.03.040)
62. Jaffe LF. 2008 Calcium waves. *Phil. Trans. R. Soc. B* **363**, 1311–1317. (doi:10.1098/rstb.2007.2249)
63. Jaffe LF. 2002 On the conservation of fast calcium wave speeds. *Cell Calcium* **32**, 217–229. (doi:10.1016/s0143416002001574)
64. Digonnet C, Aldon D, Leduc N, Dumas C, Rougier M. 1997 First evidence of a calcium transient in flowering plants at fertilization. *Dev. Camb. Engl.* **124**, 2867–2874. (doi:10.1242/dev.124.15.2867)
65. Antoine AF, Faure J-E, Cordeiro S, Dumas C, Rougier M, Feijó JA. 2000 A calcium influx is triggered and propagates in the zygote as a wavefront during *in vitro* fertilization of flowering plants. *Proc. Natl Acad. Sci. USA* **97**, 10 643–10 648. (doi:10.1073/pnas.180243697)
66. Antoine AF, Dumas C, Faure J-E, Feijó JA, Rougier M. 2001 Egg activation in flowering plants. *Sex Plant Reprod.* **14**, 21–26. (doi:10.1007/s004970100088)
67. Nakamura A, Amikura R, Hanyu K, Kobayashi S. 2001 Me31B silences translation of oocyte-localizing RNAs through the formation of cytoplasmic RNP complex during *Drosophila* oogenesis. *Dev. Camb. Engl.* **128**, 3233–3242. (doi:10.1242/dev.128.17.3233)
68. Derrick CJ, York-Andersen AH, Weil TT. 2016 Imaging calcium in *Drosophila* at egg activation. *J Vis. Exp.* **114**, e54311. (doi:10.3791/54311)